Electronic Supplementary Material (ESI) for RSC Advances
This journal is © The Royal Society of Chemistry 2013

Electronic Supporting Information

Enhanced emission of $NaYF_4$:Yb,Er/Tm nanoparticles by selective growth of Au and Ag nanoshells

Palanisamy Kannan,[a] Ferhan Abdul Rahim,[a] Teng Xue,[a] Chen Rui,[b] Handong Sun,[b] Ling Huang,[a] and Dong-Hwan Kim*[a]

[a] School of Chemical and Biomedical Engineering
[b] School of Physical and Mathematical Science
Nanyang Technological University
Singapore 637457
Phone: +65-6790 4111; Fax: +65-6791 1761
Email: dhkim@ntu.edu.sg

This journal is © The Royal Society of Chemistry 2013

Experimental section

Chemicals

Y_2O_3, Yb_2O_3 Tm_2O_3, Er_2O_3 (purity >99.9%), trifluoroacetic acid, oleic acid, 1-octadecene, sodium trifluoroacetate, polyacrylic acid and polyamidoamine generation 1 (PAMAM G1) were purchased from the Sigma-Aldrich. Cyclohexane and ethanol were supplied by Merck, Singapore. All other chemicals used in this investigation were of analytical grade and were used without further purification.

Instrumentation and methods

Powder X-ray diffraction (XRD).

The crystallinity and phase purity of the products were examined via XRD using a Bruker AXS D8-advance X-ray diffractometer with Cu Kα radiation (λ=1.5418 Å), at an operating voltage and current of 40 kV and 40 mA, respectively. The 2θ range used was from 0 to 80° in steps of 0.02°, with a count time of 2 s.

Transmission electron microscopy (TEM).

The size and morphology of the products were observed by using the JEOL JEM-1200EX transmission electron microscope with a tungsten filament at an accelerating voltage of 100-120 kV. The samples were prepared by dropping 2 µl of colloidal nanoparticles solution onto a carbon-coated copper electron microscope grid, which was allowed to dry for a few hours.

Fluorescence spectroscopy.

The photoluminescence (PL) measurements were performed using Horiba Jobin Yvon-FluoroMax-4 at room temperature. A continuous wave (CW) diode laser

emitting at 980 nm with power 2 W was used as the PL excitation source and the signal was dispersed by a 750 mm monochromator combined with suitable filters and detected by a photomultiplier by using the standard lock-in amplifier technique.

UV-Vis, FT-IR and zeta potential measurements.

All UV spectra were obtained using a UV spectrophotometer (UV-2540, Shimadzu, Kyoto, Japan). The chemical structures of the nanomaterials were analyzed by using Fourier Transform Infrared Spectroscopy (FT-IR, Bruker EQUINOX 55 Duroscope). The resolution of the spectra was 4 cm^{-1} and 100 scans were done. Solution-based ζ-potential measurement was obtained using a ζ-potential analyzer (Nano-ZS Zetasizer with DTS Nano Software, Malvern Instruments, Malvern, UK).

Synthesis of $NaYF_4$:Yb, Er/Tm nanoparticles

Caution: It should be noted beforehand that the decomposition of the metal trifluoroacetates produces various fluorinated and oxyfluorinated carbon species such as trifluoroacetic anhydride $(CF_3CO)_2O$, trifluoroacetyl fluoride CF_3CF_2COF, carbonyl difluoride COF_2 and tetrafluoroethylene C_2F_4. These species are considered heavily toxic and as such the reaction should be carried out in a well-ventilated hood. Care should also be exercised as not to inhale any of the evolved gases from the reaction.

The UCNPs were synthesized by a slight modification of John A. Capobianco and co-workers method.[29] In a typical procedure, 0.975 mmol of yttrium(III) oxide (Y_2O_3, 99.99%), 0.25 mmol of ytterbium(III) oxide (Yb_2O_3, 99.9%) and 0.026 mmol of each thulium(III) oxide (Tm_2O_3, 99.9%) and erbium (III) oxide (Er_2O_3, 99.9%) were dissolved in 10 mL trifluoroacetic acid (TFA, 99%) in a 100 mL three-necked flask. The slurry was then heated to 80°C with vigorous magnetic stirring under

vacuum for 30 min to remove water and excessive TFA. Next, 2.5 mmol sodium trifluoroacetate ($NaCOOCF_3$, 98%) was added along with 3.5 mL of oleic acid (OA, 90%) and 7.5 mL of 1-octadecene (ODE, 90%) at 100°C. Afterwards, the solution was heated to 330°C with a rate of 30°C min^{-1} and maintained at 330°C for 120 min. At approximately 250 ^{o}C, the evolution of small gas bubbles was observed from the solution indicating the decomposition of the metal trifluoroacetates. A burst of nucleation was observed between 280-300 ^{o}C which resulted in the solution becoming turbid. Subsequently, the mixture was allowed to cool to room temperature during which time the solution became clear and a yellow colloidal solution was obtained. The nanocrystals were precipitated by the addition of hexane/acetone (v/v in 1:4) and isolated via centrifugation at 3000 rpm corresponding to a relative centrifugal field (RCF) of approximately 1000. The resulting pellet was then washed once with ethanol and further purified by dispersing in a minimum amount of chloroform and precipitated with excess ethanol. The resulting nanocrystals were dried under vacuum for a minimum of 24 hrs. The resulting nanocrystals could be dispersed in non-polar solvents (e.g. hexane, toluene, dichloromethane) by sonicating a suspension of the nanocrystals in a bath sonicator for ~20 min. Adding one or two drops of oleic acid to the suspension aid in the dispersion of the nanocrystals. To eliminate this addition of oleic acid, it was preferable to leave the nanocrystals in a 'muddy' state instead of the dry powder form.

Figure S1A and B show typical scanning electron microscopy (SEM) and transmission electron microscopy (TEM) images of the $NaYF_4$:20%Yb, 2%Er/Tm nanocrystals. The well-dispersed particles suggest that the long-chain oleylamine ligand on the crystal surface prevented aggregation. The average diameter of the nanocrystals, obtained by random measurements of 100 particles from three

TEM/SEM images, is 30 nm with a standard derivation of ±2 nm. It has been reported previously,[7, 37] the emission bands can easily be assigned to transitions within the 4f-4f levels of the Er^{3+} and Tm^{3+} ions. The spectrum of the $NaYF_4$: 20% Yb, 2% Er sample exhibits the green emissions between 510 and 530 nm and between 530 and 570 nm were assigned to the $^2H_{11/2} \rightarrow {}^4I_{15/2}$ and $^4S_{3/2} \rightarrow {}^4I_{15/2}$ transitions, respectively. The red emission was observed between 635 and 700 nm originating from the $^4F_{9/2} \rightarrow {}^4I_{15/2}$ transition as well as a weak NIR emission between 830 and 860 nm corresponding to the $^4S_{3/2} \rightarrow {}^4I_{13/2}$ transition. The spectrum of the $NaYF_4$: 20% Yb, 2%Tm sample, the emission bands observed in the violet, blue region of the spectrum between 410 and 480 nm was assigned to the $^1D_2 \rightarrow {}^3F_4$ and $^1G_4 \rightarrow {}^3H_6$ transitions. A very week red emission between 640 and 670 nm and notably a NIR emission between 780 and 830 nm were assigned to the $^1G_4 \rightarrow {}^3F_4$ and $^3H_4 \rightarrow {}^3H_6$ transitions, respectively. In the present work, the upconversion spectrum of 1 wt % solution of $NaYF_4$: 20% Yb, 2%Er/Tm nanocrystals in cyclohexane under 980 nm laser diode operating with low excitation power density (2 W/cm^2) is shown in Figure S1C. The spectrum of the $NaYF_4$: 20% Yb, 2% Er/Tm sample exhibits the green emissions between 510 and 530 nm, and between 530 and 570 nm, along with the additional emission bands in the violet and blue regions of the spectrum between 410 and 480 nm due to additional doping of Tm in the same nanoparticles. The total luminescence appears yellowish-blue-green due to a combination of blue, green and red emissions from the Er^{3+} and Tm^{3+} ions.

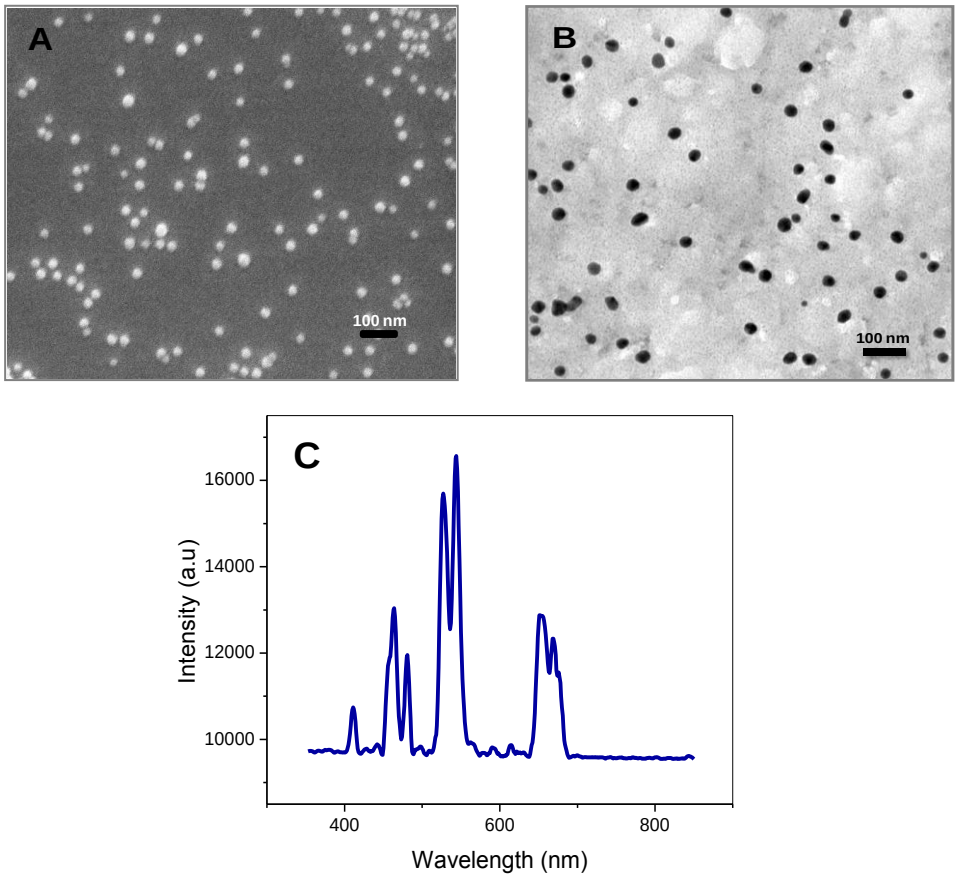

Figure S1. FE-SEM (A) and TEM (B) images of as-synthesized $NaYF_4$:Yb,Er/Tm UCNPs. (C) The corresponding fluorescence spectrum of as-synthesized $NaYF_4$:Yb,Er/Tm UCNPs.

Surface modification of up-conversion nanoparticles

A ligand exchange process was performed using poly (acrylic acid) (PAA, Mw = 1,800) as a multidentate ligand which displaces the original hydrophobic ligands on the UCNP surface by mixing together 10 mL PAA solution in ethanol (~1 wt %) and 5 mL of UCNP dispersion in chloroform (~1 wt %) with 12h stirring. The solution was then centrifuged at ca.7,000 rpm for ~60 min. After being washed three times with ethanol, the particles can be re-dispersed easily in water. After the PAA modification, the UCNPs were then sequentially rinsed with ethanol and distilled water and immersed in a mixed solution of 0.01 M EDC and 0.005 M NHS for 2h. After this treatment, the nanoparticles were thoroughly rinsed with deionized water. A

solution of 0.5mM PAMAM-G1 in ethanol was then immediately injected into the UCNPs and was further incubated for 2h. The functionalized UCNPs were stored at 4°C until further use.

FT-IR studies were performed to confirm that surface modification of the UCNPs was successful. The FT-IR spectrum in Figure S2A presented the oleic acid terminated UCNPs as having a broad band at ~3450 cm^{-1}, corresponding to O-H stretching vibration and a strong $-CH_3$ bands at 2925 and 2854 cm^{-1}. The bands at 2924 and 2854 cm^{-1} correspond to the asymmetric (V_{as}) and symmetric (V_s) stretching vibrations of methylene ($-CH_2$) in the long alkyl chain group. In addition, the bands at 1593 and 1391 cm^{-1} are assigned to the asymmetric and symmetric stretching vibration of the carboxylic group (–COOH) of the bound oleic acid in the UCNPs. After the PAA ligand exchange reaction, the decrease of the alkane peaks and the appearance of a strong carbonyl peak at 1716 cm^{-1} suggest that ligand exchange was successful (Figure S2B). Upon attachment of PAMAM G1 dendrimer (Figure S2C), the decreased carbonyl peak as well as the inconspicuous peak located at 739 cm^{-1} indicates the existence of additional N-H bonds. During the amine functionalized PAMAM G1 dendrimer modification process, the surface charge of the UCNPs is altered from negative (ζ = -20 mV) to positive (ζ = +36 mV), confirming that the amine functionalized PAMAM G1 dendrimers have been successfully grafted onto these nanoparticles. The existence of amine groups provides a powerful claw for the $NaYF_4$: Yb,Er/Tm nanoparticles to grab gold (or silver) nanoseeds, by the strong coordination between the gold and the $-NH_2$ groups.

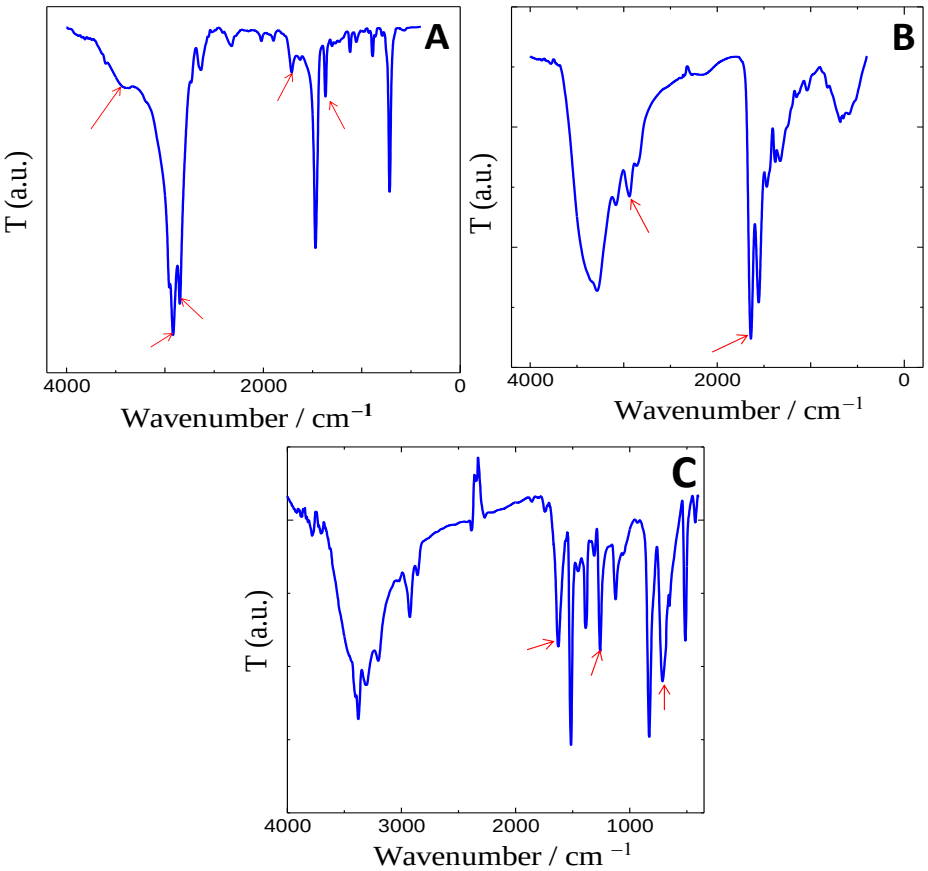

Figure S2. FT-IR spectra of UPNPs before (A) and after surface modification of PAA (B) and PAMAM G1 dendrimer (C). The FT-IR studies were performed to confirm that surface modification of the UCNPs was successful.

Attachment of gold /or silver nanoseeds as the nucleation agents for growth of gold nanoshells

The gold nanoseeds used as seeds were prepared[38] by reducing chloroauric acid with sodium boronhydride ($NaBH_4$). In brief, into 100 ml of deionized water, 2 ml of 1.0 wt % sodium citrate

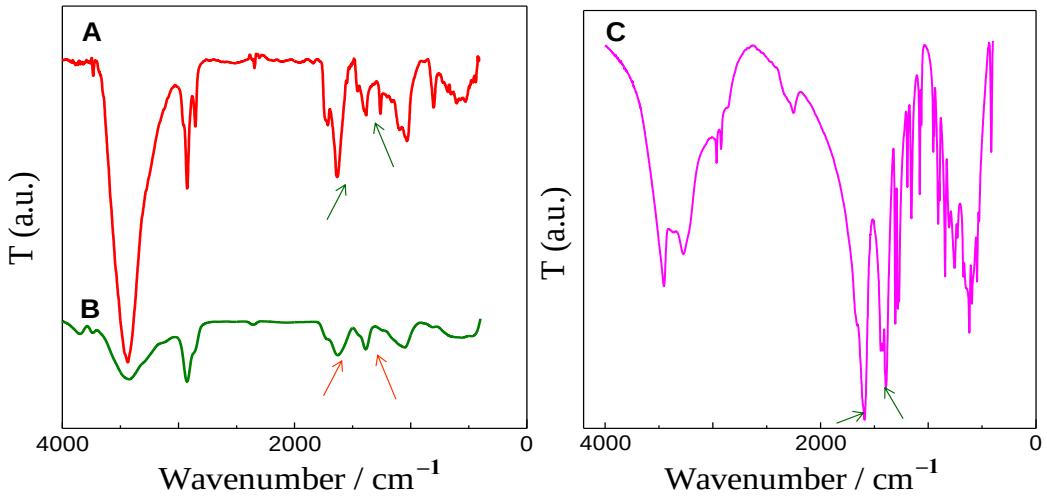

Figure S3. FT-IR spectra of UPNPs surface after embedded with gold (A) and silver (B) nanoseeds. The FT-IR spectrum "C" represents the bare trisodium citrate as the reference material for the identification of carboxylate ions.

solution was added and stirred for 3 min. 1 ml of 1.0 wt % $HAuCl_4 \cdot 3H_2O$ was then added and stirred for another 5 min. Thereafter, 1 ml of 0.1% $NaBH_4$ solution, prepared by dissolving $NaBH_4$ into 1.0 wt % sodium citrate solution, was quickly injected and the reaction was allowed for 10 min under rapid stirring. The similar protocol was followed for the synthesis of silver nanoseeds. Then the sodium citrate stabilized gold nanoseeds were successfully prepared and stored at 4°C for next application. By combining 5 mL of PAMAM G1 coated upconversion NC solution with 20 µL of gold nanoseed solution (for Ag nanoseed case, 30 µL seed solution), the gold seeds could be embedded onto the PAMAM G1 functionalized UCNP surface through electrostatic interaction.

The self-assembly of gold nanoseeds on the PAMAM coated UCNPs was further confirmed by FT-IR, measurement. Figure S3A depicts the FT-IR spectra obtained for the gold nanoseeds self-assembled on the PAMAM G1 dendrimer functionalized UCNPs show several bands, including characteristic carboxylate ion stretching modes

at 1396 cm^{-1} and 1596 cm^{-1} corresponding to symmetric and asymmetric carboxylate ion of the citrate anion, respectively.[39, 40] In contrast to the PAMAM G1 dendrimer coated UCNPs, the appearance of carboxylate ion stretching frequencies in the FT-IR spectrum for PAMAM G1 dendrimer coated UCNPs confirms the attachment of gold nanoseeds to the $–NH_2$ functionalized PAMAM surface and suggests that citrate ions stabilized the gold nanoseeds. On the other hand, the silver nanoseeds coated UCNPs presenting similar observation in the FT-IR measurements (Figure S3B) confirmed the attachment of both Au and Ag nanoseeds on the UCNPs. For the comparison, we have presented the FT-IR spectrum of bare trisodium citrate in Figure S3C, which showed strong characteristic carboxylate ion stretching modes at 1396 cm^{-1} and 1596 cm^{-1} corresponding to symmetric and asymmetric carboxylate ion of the citrate anion, respectively. For gold shell growth, seeding solution containing 5 ml of DI water, 0.3 mM of both $HAuCl_4$ and reducing agent NH_2OH were immediately added to 5 ml of the UPNPs, and incubated for ~40 min. The mild reduction was conducted under ultrasonication in an ice bath in order to prevent the UCNPs from electrostatic aggregation, as well as to lower the reaction rate to achieve well-defined nanoshell structures. Thereafter, uniformed gold nanoshell was formed by selectively reducing gold precursor onto the surface of the gold nanoseeds embedded UCNPs through a surface confined catalytic reaction of hydrogen tetrachloroaurate by hydroxylamine hydrochloride ($NH_2OH.HCl$). [41] Upon mixing, the colloidal seeding solution changed from reddish blue to brownish blue then purple over 30 min, indicating formation of gold nanoshells. For the present mode of gold nanoshell formation, the gold nanoseeds were used to enhance the colloidal stability[32, 41] of the nanoparticles.

References

1. J.-C. Boyer, F. Vetrone, L. A. Cuccia and J. A. Capobianco, *Journal of the American Chemical Society*, 2006, **128**, 7444-7445.
2. G. S. Yi and G. M. Chow, *Advanced Functional Materials*, 2006, **16**, 2324-2329.
3. Z. Li and Y. Zhang, *Angewandte Chemie International Edition*, 2006, **45**, 7732-7735.
4. K. R. Brown, D. G. Walter and M. J. Natan, *Chemistry of Materials*, 1999, **12**, 306-313.
5. S. L. Cumberland and G. F. Strouse, *Langmuir*, 2001, **18**, 269-276.
6. A. Sivanesan, P. Kannan and S. Abraham John, *Electrochimica Acta*, 2007, **52**, 8118-8124.
7. J. L. Lyon, D. A. Fleming, M. B. Stone, P. Schiffer and M. E. Williams, *Nano Letters*, 2004, **4**, 719-723.
8. L. Wang, J. Bai, Y. Li and Y. Huang, *Angewandte Chemie International Edition*, 2008, **47**, 2439-2442.